PROGRESS REPORT

NASA Grant NAGW-3374

TITLE: Shock and Thermal History of Iron and Chondritic Meteorites

PRINCIPAL INVESTIGATOR: Dr. Joseph I. Goldstein

This progress report includes our work since the last progress report of 3/27/92. Copies of the publications are attached to this proposal. Within this time period, we have had 5 papers published, 1 paper accepted for publication and 3 papers submitted for publication. Attached to the progress report are copies of the 9 papers listed below.

The published papers are:

1. "An APFIM/AEM Study of Phase Decomposition in Fe-Ni Alloys at Low Temperatures", J. Zhang, M. K. Miller, D. B. Williams and J. I. Goldstein, Surface Science, **266**, 433-440, (1992).

2. "Definition of the Spatial Resolution of X-ray Microanalysis in Thin Foils", D. B. Williams, J. R. Michael, J. I. Goldstein and A. D. Romig, Jr., Ultramicroscopy, **47**,121-132, (1992).

3. "X-ray Microanalysis and Electron Energy Loss Spectrometry in the Analytical Electron Microscope: Review and Future Directions", J. I. Goldstein and D. B. Williams, Microbeam Analysis, **1**, 29-53, (1992).

4. "Future Directions of X-ray Microanalysis in the Analytical Microscope", J. I. Goldstein, in *Electron Microscopy I*, ed K. H. Kuo and Z. H. Zhai, 5th Asia-Pacific Electron Microscopy Conference, World Scientific, 138-141, (1992).

5. "Applications of the Analytical Electron Microscope to Materials Science", J. I. Goldstein, in Micromat-92, Sociedade Brasileira de Microscopia Electronica, 1-4, (1992).

The papers accepted for publication are:

1. "Microstructure of Plessite and its Formation in Iron Meteorites", J. Zhang, D. B. Williams and J. I. Goldstein, to be published in Geochimica et Cosmochimica Acta, 1993.

The papers submitted for publication are:

1. "Phase Transformation in Fe-Ni Martensitic Alloys and Implications for the Low Temperature (<450°C) Fe-Ni Phase Diagram", J. Zhang, D. B. Williams and J. I. Goldstein, submitted to Met Trans A, 1992.

2. "Interface Reaction Controlled Precipitate Growth in Fe-Ni Martensite Decomposition: A Numerical Model and AEM Analysis", J. Zhang, D. B. Williams and J. I. Goldstein, submitted to Met Trans A, 1992.

3. "A Comparison of Metallographic Cooling Rate Methods Used in Meteorites", M. A. Herpfer, J. W. Larimer and J. I. Goldstein, submitted to Geochimica et Cosmochimica Acta, 1992.

The work statement for the second year of our present three year grant included two major projects within an overall objective entitled, "Shock and Thermal History of Iron and Chondritic Meteorites". The work statement follows.

WORK STATEMENT (Second year, 12 Months, 3/1/93 - 2/28/94)

1. Determination of the Structure and Chemistry of the Metallic Particles in Chondritic Meteorites

We will characterize the fine structure and microchemistry of metallic particles of chondrites by high resolution scanning electron microscopy, analytical electron microscopy and electron microprobe techniques. Along with phase diagram and kinetics results from our study of the Fe-Ni-S system (project 2) and studies of plessite in iron meteorites (preceding grant), it should be possible to develop the low temperature shock and thermal history of the metal particles and their host meteorites. Collaboration with the meteorite group at the University of Hawaii is crucial as both groups will work as much as possible on the same meteorites and in many cases the same thin sections. The UH group will study the silicates and opaque minerals in order to delineate the high temperature parts of the thermal history of the chondrites. Initial emphasis of both groups will be placed on ordinary chondrites, types 3-6. We expect to develop, with the UH group, thermal models for the individual chondrites which include both high and low temperature stages, and consider various levels of shock. The models must also be consistent with results of other techniques such as age dating from isotopic and track techniques.

The project will be broken into two parts: a study of the fine structure in high metamorphic grade (5,6) ordinary chondrites and a study of the fine structure in low metamorphic grade (3,4) ordinary chondrites. The difficulty of understanding the structure and the thermal history of the metal particles will increase as the degree of reheating or metamorphism decreases and we envision developing more complex thermal models for the low metamorphic grade chondrites.

In the second year of the study we will analyze, using electron microscopy techniques, metal particles in at least 3 H and 3 LL ordinary chondrites of the high metamorphic grade, 5 and 6. The LL chondrites have larger amounts of clear taenite and the H chondrites have larger amounts of metal. We will take advantage of our new AEM intrumentation (Delivery of Vacuum Generators 300 kV FEG analytical electron microscope expected mid to late 1992.) and better specimen preparation techniques to thin meteorite samples in order to improve x-ray spatial resolution to the 2.5 nm range. The samples investigated by our high resolution techniques will also be studied by our collaborators at the University of Hawaii. With their assistance, samples for use in electron microscopy will be selected and prepared. In addition, we will begin a study, with our collaborators, of the array of metal particles from sections of type 3 and 4 metamorphic grade chondrites. Mr. Cheol Yang, a Ph. D. candidate, with the assistance of Drs. D. B. Williams and J. I. Goldstein, will be responsible for this research.

2. Metal Particle Microstructure and Thermal History - Importance of the Fe-Ni-S System

We will investigate the Fe-Ni-S system by determining pertinent 2 phase tie lines and 3 phase boundaries, by performing slow cooling experiments on Fe-Ni-S alloys of chondritic meteorite composition, and by measuring pertinent ternary diffusion paths between troilite and kamacite-taenite by a diffusion couple technique. With these data we expect to gain a better understanding of how the chondrite microstructures develop, how the segregation of Ni between the kamacite, taenite and sulfide phases occurs and how Ni composition gradients in taenite formed during final cooling of the ordinary chondrites in their asteroidal bodies. With the results of our structural and chemical study (project 1) and this study we may also be able to develop a more accurate cooling rate model for determining the thermal history of the host chondrites in the temperature interval from 700 to 300°C.

In the second year of the study we will continue our experimental study of the Fe-Ni-S system using Fe-Ni-S alloys of chondritic meteorite composition and powder samples of appropriate amounts of Fe, Ni and S heat treated in the temperature range 800 to 300° C. In addition we will develop the diffusion couple technique for studying the kinetics of the growth of kamacite and taenite. Ms. Lina Ma, a Ph. D. candidate, with the assistance of Drs. D. B. Williams and J. I. Goldstein, will be responsible for this research.

These tasks have been actively pursued during the present grant period. The following sections include a summary of the PI group achievements toward the objectives/tasks outlined above. In addition, work is continuing on the development of x-ray microanalysis techniques for the analytical electron microscope.

1. Determination of the Structure and Chemistry of the Metallic Particles in Chondritic Meteorites

The preparation of thin foils of metal particles for electron microscopy from ordinary chondrites of metamorphic grade 6 was the major topic of research in this task. Some of the considerations for making adequate thin section are that the sample must be strong enough to withstand the necessary mechanical handling and thinning, both the metal particles and the matrix must be thinned at similar rates so that the matrix is thick enough to support the small sized metal particles, and a large electron transparent region in the metal particles is needed. Unfortunately we found that producing adequate thin sections was a much more difficult process than expected.

We have approached making thin sections by either slicing the chondrite and thinning the metal within that section or by crushing the chondrite to extract the metal and then thinning the metal. The sliced chondrite sample appeared to be a more appropriate starting point for the thinning process. However, more rapid thinning of the silicate by ion beam techniques leaves the metal unsupported and sample thinning cannot be completed. The crushing method also has a number of problems. For example it is not possible to completely separate metal particles from the silicate matrix and the crushing process can deform the metal. We have had success in thinning extracted metal particles using various combinations of thinning procedures including dimpling (pre mechanical grinding of the metal), electrochemical (jet) polishing and ion-beam thinning (IBT). Figure 1 shows schematic diagrams of a thin specimen preparation technique which has proved successful with metal particles.

The first analytical electron microscopy (AEM) study of metal particles in the Saint Severin, LL6 chondrite, was presented at the 24th Lunar and Planetary Science Conference, Yang et al., LPSC **XXIV**, 1557-8 (1993). A copy of the abstract follows this section. Our preliminary studies have shown the presence of the cloudy zone. The microstructure of Saint Severin cloudy zone is very similar to that of the Carlton iron meteorite and the Estherville stony-iron previously studied. Ordering is observed by superlatice spots in the electron diffraction pattern of the island phase in the cloudy zone. The presence of the tetrataenite phase was confirmed.

The nucleation and growth of tetrataenite (FeNi) in meteorites was described in a paper given at the 55th Annual Meeting of the Meteoritical Society in Copenhagen last summer (Goldstein et al. Meteoritics, **27**, 227-8, 1992). A copy of the abstract follows this section. This paper describes a common nucleation and growth process for this phase as it appears in iron, stony and stony-iron meteorites.

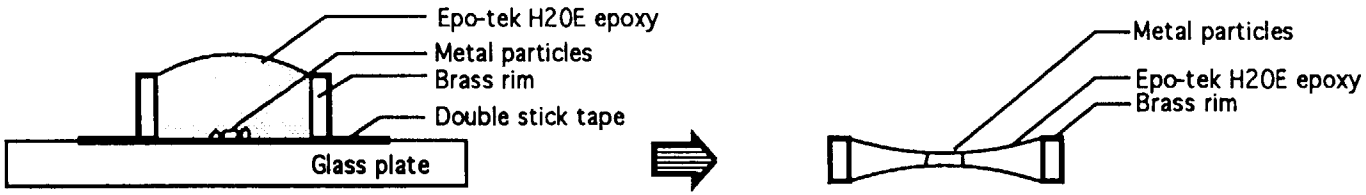

MOUNTING ⇒ GRINDING & DIMPLING

⇒ LOM & SEM OBSERVATION ⇒ 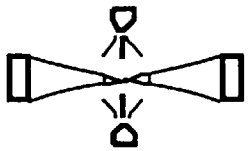 ⇒ IBT ⇔ AEM

JET POLISHING

THIN SPECIMEN PREPARATION TECHNIQUE

PRELIMINARY AEM STUDY OF THE MICROSTRUCTURE AND COMPOSITION OF METAL PARTICLES IN ORDINARY CHONDRITES ; C. W. Yang, D. B. Williams, and J. I. Goldstein, Department of Materials Science and Engineering, Lehigh University, Bethlehem, PA 18015

The purpose of this study is to examine the microstructure and composition of the metal particles in ordinary chondrites using analytical electron microscopy (AEM) techniques. Since the phases produced within the metal particles are very fine, the application of various AEM techniques for structural and chemical characterization is critical. However, thin specimen preparation for AEM study has proven very difficult because of the matrix silicate which is present. This is the first AEM study of the metal particles in chondrites. A type 6 chondrite, Saint Severin (LL6), was selected for examination because the metal phases have been reheated into the single phase taenite region (>700°C), and cooled slowly to lower temperatures. A combination of electron optical instruments was employed including a field emission gun (FEG) JEOL 840F high resolution scanning electron microscope (HRSEM), a JEOL 6300F FEG-HRSEM, a Philips 400T AEM, and a JEOL 733 electron probe microanalyzer (EPMA).

Figs. 1a and 1b are HRSEM images of a taenite particle in the Saint Severin ordinary chondrite. The taenite particle is surrounded by silicate (S). From the high Ni border moving into the particle, the microstructure includes the outer taenite rim (TR) which corresponds to clear taenite 1 (CT1) in iron meteorites (52 - 46 wt% Ni), and the cloudy zone (CZ, 45 - 30 wt% Ni). The outer taenite rim contains three sub-zones (1, 2, 3). The size of the constituents of the cloudy zone changes along the Ni concentration gradient. Fig. 1c shows further high magnification image of the center of the cloudy zone. The microstructure shown in Fig. 1 is consistent with the observation of Duffield[1]. The microstructure and the chemistry are closely related to each other.

Fig. 2a is a transmission electron microscope (TEM) bright field image of the cloudy zone in Saint Severin. The average Ni content of this region is 37 wt% Ni. Comparing the size of the phases with the HRSEM image (Fig.1c) and Ni content determined by EPMA, this region is also in the middle of the cloudy zone. The CZ region in the taenite particles contains two phases.The structure of the cloudy zone of Saint Severin is very similar to that of Carlton iron meteorite and Estherville stony-iron meteorite as investigated by Zhang[2] and Reuter[3], respectively. The cloudy zone forms by spinodal decomposition[3]. According to a recent Fe-Ni phase diagram[4], the taenite in the composition range from 41 wt% Ni to 28 wt% Ni transforms spontaneously into Ni-rich regions (light regions in Fig. 2a, island phase) and Ni-poor regions (dark regions in Fig. 2a, honeycomb phase) defined by the miscibility gap. The Ni-rich region undergoes the ordering transformation and forms tetrataenite. As the temperature decreases, the Ni-poor region decreases in Ni content and transforms to martensite. The selected area diffraction (SAD) pattern (Fig. 2c), as indexed in Fig. 2d, is composed of the fcc <110> zone axis pattern, two bcc <111> zone axis patterns which are in a twinning orientation relationship, and weak superlattice diffraction spots which can be observed on the negative although they are not clear on the print. The superlattice spot is due to the ordering of the parent fcc phase to tetrataenite. The twinning plane is $(002)_{fcc}$. The centered dark field (CDF) image (Fig. 2b) taken from a $(0\bar{1}1)$ bcc spot in Fig. 2c shows that the honeycomb phase has a bcc structure. The microstructure of other taenite particles in Saint severin will also be described.

References [1] Duffield C.E., Williams D.B., and Goldstein J.I. (1991) *Meteoritics* , *26* , 97 [2] Zhang J. (1991) *Ph.D Dissertation, Lehigh Univ.* [3] Reuter K.B., Williams D.B., and Goldstein J.I. (1988) *Geochim. Cosmochim. Acta* , *52* , 617 [4] Reuter K.B., Williams D.B., and Goldstein J.I. (1989) *Met. Trans., 20A* , 719

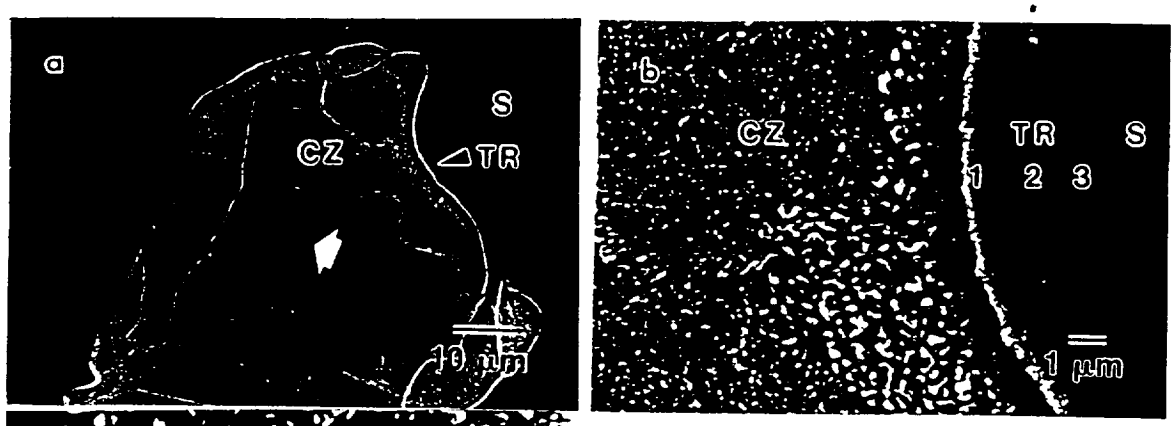

Fig. 1 a), b) HRSEM micrographs of taenite particle in Saint Severin (LL6) chondrite. c) HRSEM micrograph of the center of cloudy zone indicated by arrow in a)

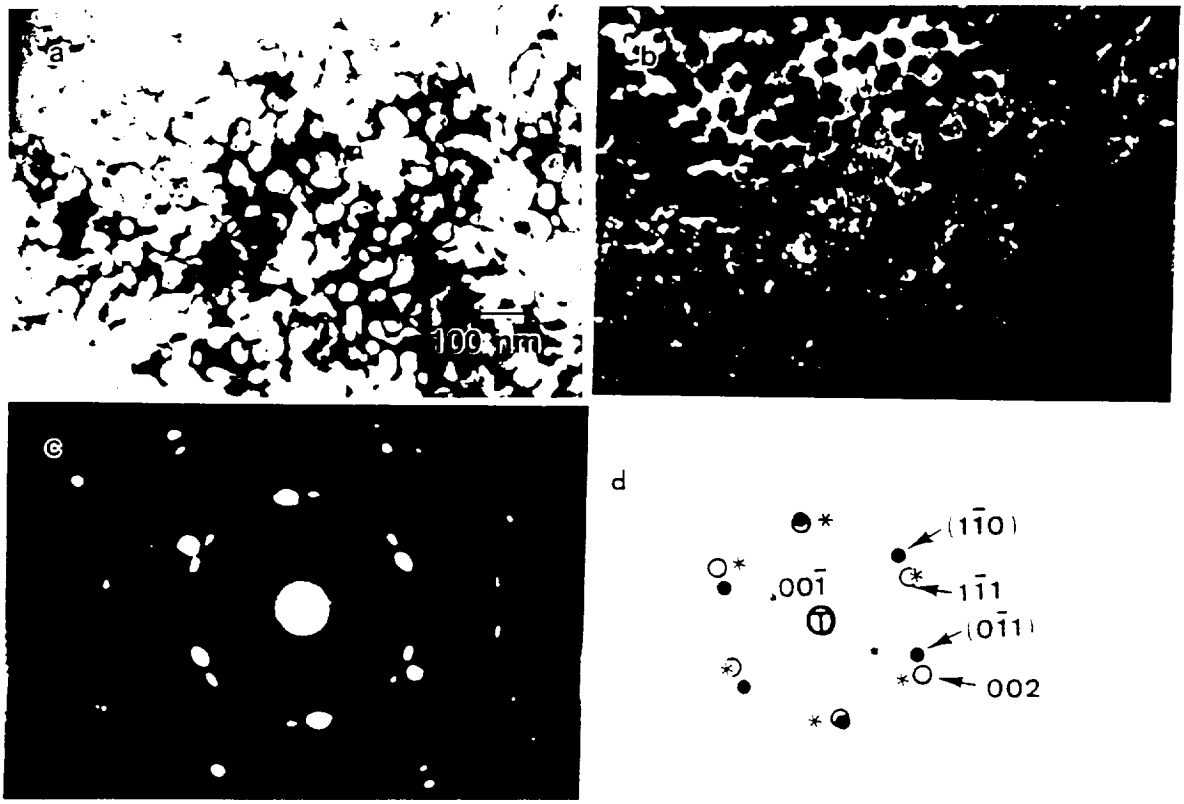

Fig. 2 a) TEM bright field image of CZ region of Saint Severin chondrite, b) centered dark field image from a (0$\bar{1}$1) bcc spot, c) SAD pattern, d) indexing of SAD pattern; ● hkl: bcc[111] zone axis pattern; * hkl: another bcc[111] zone axis pattern; O hkl: fcc[110] zone axis pattern; • superlattice diffraction spots (observed on the negative)

be totally immune from the acid attack: only three ppm remain from the original concentration of eight ppm in the whole-rock meteorite.

N_C has still not been identified, but is further operationally defined. The combustion temperature of N_C in the acid-resistant residue constrains its identification: nitrogen present as Si_3N_4 or substituted in SiC does not seem likely, unless the minerals are extremely fine-grained or exceptionally radiation-damaged. It is possible that N_C is hosted by a mineral not previously suggested as a pre-solar grain, assuming that the ^{15}N-enrichments described are indicative of such an origin. The more complex problem of how isotopically heavy nitrogen is so completely distributed throughout the meteorite may become more easy to address once the most likely source of the ^{15}N-enrichment is positively identified. One possibility is that parent-body processing, including shock, degassed a component of interstellar origin, which subsequently exchanged with or nitrified other phases.

Grady M. M. and Pillinger C. T. (1992) *Earth Planet. Sci. Lett.* (submitted).

Cosmic-ray exposure history of enstatite meteorites. Th. Graf and K. Marti. Dept. of Chemistry, Univ. of California, San Diego, La Jolla, California 92093-0317, USA.

Enstatite achondrites display long exposure ages (T_e) compared to the collisional lifetimes of ordinary chondrites of ~17 Ma (Eberhardt *et al.*, 1965; Graf and Marti, 1992), and therefore suggest special orbits for these meteorites. Recently, Gaffey *et al.* (1992) suggested a link between aubrites, near-Earth asteroid 3103 and E-type steroids of the Hungaria family, based on spectral matches and orbital considerations. This would represent the first direct link of a meteorite type and an asteroid family. Moreover, the orbital elements of Apollo object 3103 are consistent with long collisional lifetimes as observed for the Norton County and Mayo Belwa aubrites (T_e = 110–120 Ma). There has been much debate over the genetic relation between E-chondrites and aubrites (Keil, 1989). Crabb and Anders (1981) found that exposure ages show a pronounced trend E4 < E6 < aubrites. We reevaluate the cosmic ray record of enstatite meteorites based on an updated database (Schultz and Kruse, 1989) as well as improved production rates and shielding corrections. We make the following observations: 1) Five out of 11 aubrites cluster at T_e = 55 ± 5 Ma. All three known solar gas bearing aubrites belong to this group, lending considerable support to the reality of a discrete event at this time. 2) While Gaffey *et al.* (1992) suggested that a significant fraction of aubrites may derive from 1–2 meteorite streams, the average $^{22}Ne/^{21}Ne$ ratios of ~1.11 and saturated ^{26}Al activities render a long 2π irradiation interval preceding the (short) 4π exposure in space unlikely. 3) In a $^{38}Ar/^{21}Ne$ *vs.* $^{22}Ne/^{21}Ne$ diagram, the inferred spallation ratios of EH-chondrites plot systematically below the expected correlation line. However, Cl abundances in EH-chondrites are about an order of magnitude larger than those in ordinary chondrites. If significant amounts of ^{36}Ar produced by the reaction $^{35}Cl(n, \gamma)^{36}Cl \rightarrow {}^{36}Ar$ are present, the standard procedure overestimates trapped Ar. Indeed, $^{36}Ar/^{38}Ar$ ratios of ~7 were observed in stepped heating experiments of Abee separates, indicating the presence of such a component (Wacker, 1982). We calculate a ratio of $^{36}Ar(n, \gamma)/^{36}Ar(sp)$ of 1.7–2.6 from the observed shifts in the 3-isotope plot. Since concentrations of (n, γ) products are predicted to increase with shielding more steeply than spallation products, it is surprising that the calculated $^{36}Ar(n, \gamma)/^{36}Ar(sp)$ ratios are rather constant over a wide range of shielding conditions. Alternatively, matrix effects (enhanced cascade of secondary GCR particles in high Z targets), previously suggested for mesosiderites (Begemann and Schultz, 1988) are also evaluated. 4) Five out of 11 EH-chondrites have exposure ages <4 Ma. This indicates either a recent break-up or very short lifetimes. In contrast, 6 of 10 EL-chondrites cluster at T_e = 30 ± 3 Ma, indicating a collisional event at this time. Only one EL-chondrite has an exposure age <27 Ma.

The exposure age systematics show that discrete collisional events are at least as common for enstatite meteorites as for ordinary chondrites (Marti and Graf, 1992). The systematics do not suggest an origin off the same immediate parent object. However, differential orbital evolution following an early catastrophic disruption of a parent asteroid can not presently be discounted, except that the solar wind loading of aubrites requires the evolution of a regolith. The high retention of radiogenic $^{40}Ar_r$ rule against major heat pulses in the recent history.

Begemann F. and Schultz L. (1988) *Lunar Planet. Sci.* (abstract) **19**, 51–52.

Crabb J. and Anders E. (1981) *Geochim. Cosmochim. Acta* **45**, 2443–2464.

Eberhardt P., Eugster O. and Geiss J. (1965) *J. Geophys. Res.* **70**, 4427–4434.

Gaffey M. J., Reed K. L. and Kelley M. S. (1992) *Lunar Planet. Sci.* (abstract) **23**, 395–396.

Graf Th. and Marti K. (1992) *Lunar Planet Sci.* (abstract) **23**, 433–434.

Keil K. (1989) *Meteoritics* **24**, 195–208.

Marti K. and Graf Th. (1992) *Ann. Rev. Earth Planet. Sci.* **20**, 221–243.

Schultz L. and Kruse H. (1989) *Meteoritics* **24**, 155–172.

Wacker J. F. (1982) Ph.D. thesis, Univ. of Arizona.

Nucleation and growth of tetrataenite (FeNi) in meteorites. J. I. Goldstein,[1] D. B. Williams,[1] and J. Zhang.[2] [1]Materials Science and Engineering, Lehigh University, Bethlehem, Pennsylvania 19015, USA. [2]3M Corporation, St. Paul, Minnesota 55144, USA.

The mineral tetrataenite (ordered FeNi) has been observed in chondrites, stony irons and iron meteorites (Clarke and Scott, 1980). FeNi is an equilibrium phase in the Fe-Ni phase diagram (Fig. 1) and orders to tetrataenite at ~320 °C (Reuter *et al.*, 1989). The phase forms at temperatures at or below the eutectoid temperature (~400 °C) where taenite (γ) transforms to kamacite (α) plus FeNi (γ'). An understanding of the formation of tetrataenite can lead to a new method for determining cooling rates at low temperatures (<400 °C) for all types of meteorites.

In a recent study of plessite in iron meteorites (Zhang *et al.*, 1992a), two transformation sequences for the formation of tetrataenite were observed. In either sequence, during the cooling process, the taenite (γ) phase initially undergoes a diffusionless transformation to a martensite (α, bcc) phase without a composition change. The martensite then decomposes either *above* or *below* the eutectoid temperature (~400 °C) during cooling or upon subsequent reheating.

During martensite decomposition *above* the eutectoid, the taenite (γ) phase nucleates by the reaction $\alpha_2 \rightarrow \alpha + \gamma$ and grows under volume diffusion control. The Ni composition of the taenite increases continuously following the equilibrium $\gamma/\alpha + \gamma$ boundary while the Ni composition of the kamacite matrix decreases following the $\alpha/\alpha + \gamma$ phase boundary (Reuter *et al.*, 1989), see Fig. 1. Below the eutectoid temperature, the precipitate composition follows the equilibrium $\gamma'/\alpha + \gamma'$ boundary and reaches ~52 wt% Ni, the composition of FeNi, γ'. The kamacite (α) matrix composition approaches ~4 to 5 wt% Ni. The ordering transformation starts at ~320 °C forming the tetrataenite phase.

During martensite decomposition *below* the eutectoid temperature, FeNi should form directly by the reaction $\alpha_2 \rightarrow \alpha + \gamma'$ (FeNi). If this transformation sequence occurs, then the composition of kamacite and tetrataenite should also be given by the $\alpha/\alpha + \gamma'$ and $\gamma'/\alpha + \gamma'$ boundaries of the Fe-Ni phase diagram (Fig. 1). However, the Ni content of kamacite and tetrataenite in black plessite, which forms below 400 °C, is ~10 wt% in kamacite and ~57 to 60 wt% in tetrataenite, much higher than the values given by the equilibrium phase diagram (Zhang *et al.*,

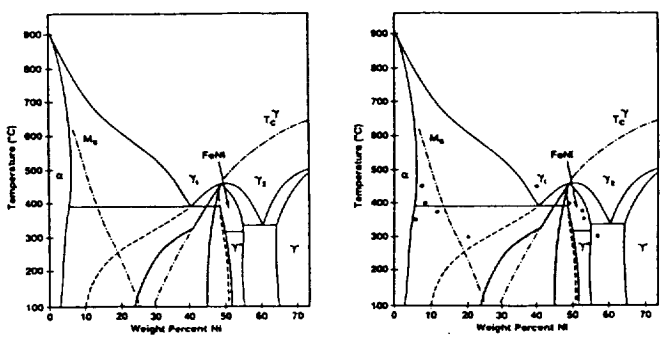

Fig. 1. (Left) Fe-Ni Phase Diagram (Reuter *et al.*, 1989).
Fig. 2. (Right) Measured FeNi composition from heat treated alloys (Zhang *et al.*, 1992b).

1992a). It has been observed experimentally (Zhang *et al.*, 1992b) that the Ni composition of the γ phase formed by martensite decomposition below 400 °C lies along a metastable extension of the high temperature $\gamma/\alpha + \gamma$ phase boundary, Fig. 2. Therefore, the FeNi phase formed by α_2 decomposition below 400 °C has a non-equilibrium Ni content, > 50 to 56 wt%. The growth or thickening of the FeNi phase occurs by some combination of interface and diffusion control (Zhang *et al.*, 1992a).

CLARKE R. S. AND SCOTT E. R. D. (1980) *Amer. Mineral.* **65**, 624–630.

REUTER K. B., WILLIAMS D. B. AND GOLDSTEIN J. I. (1989) *Met. Trans.* **20A**, 719–725.

ZHANG J., WILLIAMS D. B. AND GOLDSTEIN J. I. (1992a) *Geochim. Cosmochim. Acta* (submitted).

ZHANG J., WILLIAMS D. B. AND GOLDSTEIN J. I. (1992b) *Met Trans.* (submitted).

Trace and major element chemistry across the Cretaceous/Tertiary boundary at Stevns Klint. G. Graup and B. Spettel. Max-Planck-Institut für Chemie, Abteilung Kosmochemie, Saarstrasse 23, D-6500 Mainz, Germany.

INAA measurements of samples obtained by high resolution stratigraphy on a mm scale reveal considerable variations in element concentrations across the boundary with their respective maxima stratified in distinct sublayers (Graup *et al.*, 1992). These results suggest that measurements of bulk boundary samples a few cm thick may be inappropriate as concentration variations and element ratios would be leveled out pretending a single geochemical signal. Having investigated a sample comprising sublayers B, C, and D (Fig. 1), Alvarez *et al.* (1980) acknowledge that "no information is available on the chemical variations within the boundary." This kind of information is given below and shown in Fig. 1 (sublayers A and B are drafted in double scale).

From the main lithologic characteristics of Maastrichtian to Paleocene sediments (Schmitz, 1988; Graup *et al.*, 1992) it is readily deduced that Eh and pH conditions in the marine environment changed from oxic-mildly alkaline with normal carbonate sedimentation (Q-M) to anoxic-(mildly) acid with deposition of pyrite spherules (A3), organic material, and clay minerals in the Fish Clay (A-D), followed by a restoration of oxic-alkaline conditions depositing the Cerithium limestone (E-I). The element distribution across the boundary obviously mirrors these alternating environmental conditions: compounds soluble under acid and reducing conditions like Ca-carbonate and Mn are strongly depleted in the Fish Clay (Fig. 1A), whereas compounds stable and insoluble under these conditions are highly enriched (Fig. 1B). The opposite holds true for the calcareous sediments.

Across the boundary, enhanced element concentrations are not evenly distributed but appear to be stratified with maximum concentrations in three distinct sublayers for the following elements: (1) Al (hard clay): peak concentrations for REE (La 72 ppm) and U (45.5 ppm) as compared to 13 ppm La and 2 ppm U in sublayer A2 immediately above. (2) A3 (pyrite spherules): peak concentrations for Fe, Co, Ni, Au, and all chalcophiles. The trace elements correlate well with Fe across the boundary. (3) B (organic-rich marl): peak concentrations for Ir (87.6 ppb), Re (96 ppb, but 113 ppb in C), and organic carbon (2.3%). Ir correlates well with organic carbon (data from Schmitz, 1988), to a lesser extent with Re and, possibly, Os, but is not correlated with Ni, Co or Au (Graup *et al.*, 1992).

Despite large variations in absolute concentrations and, therefore, also of ratios for elements with differing chemical behaviour, there are some pairs of chemically closely related elements (siderophiles as well as chalco- and lithophiles), the ratios of which remain fairly constant over the whole boundary range. Examples shown in Fig. 1A: Ni/Co (average 7.6/SD 1.2) and La/Yb (12.9/SD 2.4). Although Eh, pH conditions vary widely, these elements are not fractionated from each other because of their closely similar geochemical behaviour.

The high concentrations of Ir, Ni, and chalcophile elements making up the K/T geochemical anomaly should be indicative of an external component added to the marine environment. The elements introduced were subsequently precipitated according to their chemical properties and changing Eh, pH conditions resulting in stratification of peak concentrations. The constancy of certain element ratios indicates an extended period of availability for this external component.

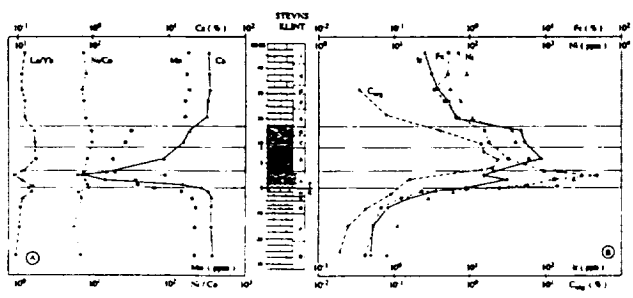

ALVAREZ L. W., ALVAREZ W., ASARO F. AND MICHEL H. V. (1980) *Science* **208**, 1095–1108.

GRAUP G., PALME H. AND SPETTEL B. (1992) *Lunar Planet. Sci.* (abstract) **23**, 445.

SCHMITZ B. (1988) *Geology* **16**, 1068–1072.

Not all refractory spherules in CM2s are chondrules. R. C. Greenwood. Department of Mineralogy, Natural History Museum, Cromwell Road, London SW7 5BD, UK.

Refractory spherules in CM2 meteorites are small, <300 μm diameter, inclusions composed predominantly of spinel, with accessory hibonite and perovskite (Macdougall, 1981). On the basis of their chondrule-like morphology, and the inward-radiating habit of hibonite in some inclusions, it has been suggested that refractory spherules formed from liquid droplets (Macdougall, 1981; MacPherson *et al.*, 1983). Since many spherules are composed purely of spinel Macdougall (1981) estimated that their one-atmosphere melting temperature might have been as high as 2135 °C. Melt temperatures in excess of 1550 °C were estimated by MacPherson *et al.* (1983) for the spinel-hibonite spherule BB1.

Refractory spherules are a minor component of the Ca-Al rich inclusions (CAIs) found in CM2s. Of 345 CAIs located in the CM2 Cold Bokkeveld only four are refractory spherules (study in collaboration with M. Lee, University of Essex). Textural evidence from Cold Bokkeveld demonstrates that CAIs in CM2s are highly fragmented and must have been derived by disruption of larger objects (Greenwood *et al.*, 1991). That this is also the case for refractory spherules is clearly demonstrated by MSP1, an anhedral, spinel-bearing inclusion (300 μm longest dimension) located *in situ* in Murchison (CM2). It comprises a rounded core (110 μm diameter) of Fe-free spinel (V_2O_3 0.5 wt%) surrounded by a rim of pyroxene (15–25 μm thick), in turn enclosed by a zone of olivine ($Fo_{99.7}$) and Mg-rich phyllosilicate. The spinel core contains 15% void space (estimated). The pyroxene rim is zoned outwards from fassaite to diopside. Blocky crysyals of olivine <20 μm diameter, form a discontinuous rim to pyroxene and occur as isolated grains enclosed by Mg-phyllosilicate. The inclusion has an irregular outline and a sharp contact with surrounding matrix, indicating that it is a fragment of a larger, now disrupted CAI.

In CV3 meteorites, refractory spinel-rich spherules, similar to the Murchison example, occur within a number of different inclusion-types. Nodules, 5–300 μm diameter, composed of spinel, melilite, perovskite and pyroxene are common constituents of amoeboid olivine aggregates (Hashimoto and Grossman, 1987). Melilite is also present in some Murchison spherules (MacPherson *et al.*, 1983), and prior to aqueous alteration may have been an important constituent in many of these objects. Spherical clumps of spinel crystals, termed "framboids" by El Goresy *et al.* (1979) are common constituents of Type B2 coarse-grained CAIs (Wark and Lovering, 1982). One B2 CAI in Vigarano contains a 160 μm diameter "framboid" with a 10–20 μm thick rim of spinel enclosing a touching framework of rounded grains (5–15 μm diameter). Melilite, present in the bulk inclusion, forms an outer rind in the "framboid" 5–10 μm thick and may be contiguous with crystals($Åk_{16.5}$) interstitial to spinel within the "framboid." Individually rimmed spinel nodules, up to 300 μm in diameter, are also an important component of "Fluffy" Type A inclusions (MacPherson and Grossman, 1984).

The structure of the Murchison inclusion MSP1 indicates that at least some CM2 refractory spherules were components of larger inclusions.

17.

2. Metal Particle Microstructure and Thermal History - Importance of the Fe-Ni-S System

Progress is being made on determining tie lines in our experimental study of the Fe-Ni-S system. Our first objective is to determine the phase relations between kamacite, taenite and FeS in the temperature range 900 to 300°C. We are using two approaches: 1) solid samples produced by melting, solidification, homogenization and heat treatment at tempreature, and 2) powder samples produced by powder processing at the temperature of interest. The second approach was the traditional one used for the measurement of the current phase diagram (Kullerod, 1963). Preliminary results have indicated that the first approach yields reproducible measured tie lines at high temperatures, 900°C.

At this time we have obtained adequate purity alloys, built an apparatus to melt Fe-Ni-S alloys in a reducing atmosphere, secured the necessary high temperature furnaces, and heat treated a number of alloys. We have also established several tie lines between taenite and troilite at 900 and 800°C using electron probe microanalysis of heat treated (previously melted) Fe-Ni-S alloys. Figure 2 shows the isothermal diagram of the Fe-Ni-S system at 900°C by Kullerud. Four of our measured γ + FeS tielines are shown on the diagram. These data indicate that the γ + FeS phase field is more extensive than that given in the Kullerud diagram and that the γ + FeS + L field probably is stable at higher Ni contents.

In addition, preliminary work has begun on developing analytical techniques so that the AEM can be used to measure tie lines at lower temperatures where diffusion will be limited and interface measurements will require x-ray spatial resolutions much better than 1mm. This study is progressing well and we look forward to lower temperature phase diagram results in the near future.

3. Additional Program Activities: X-ray Microanalysis in the Analytical Electron Microscope

During the present grant period we have continued to develop our capabilities in the x-ray microanalysis area, anticipating the time when we will be able to analyze thin sections of metal particles from chondrites. We have written several papers discussing methods to improve x-ray microanalysis and spatial resolution in the analytical electron microscope. These papers are given below and are included in the progress report.

1. "Definition of the Spatial Resolution of X-ray Microanalysis in Thin Foils", D. B. Williams, J. R. Michael, J. I. Goldstein and A. D. Romig, Jr., Ultramicroscopy, **47**,121-132, (1992).

2. "X-ray Microanalysis and Electron Energy Loss Spectrometry in the Analytical Electron Microscope: Review and Future Directions", J. I. Goldstein and D. B. Williams, Microbeam Analysis, **1**, 29-53, (1992).

3. "Future Directions of X-ray Microanalysis in the Analytical Microscope", J. I. Goldstein, in *Electron Microscopy I*, ed K. H. Kuo and Z. H. Zhai, 5th Asia-Pacific Electron Microscopy Conference, World Scientific, 138-141, (1992).

4. "Applications of the Analytical Electron Microscope to Materials Science", J. I. Goldstein, in Micromat-92, Sociedade Brasileira de Microscopia Electronica, 1-4, (1992).

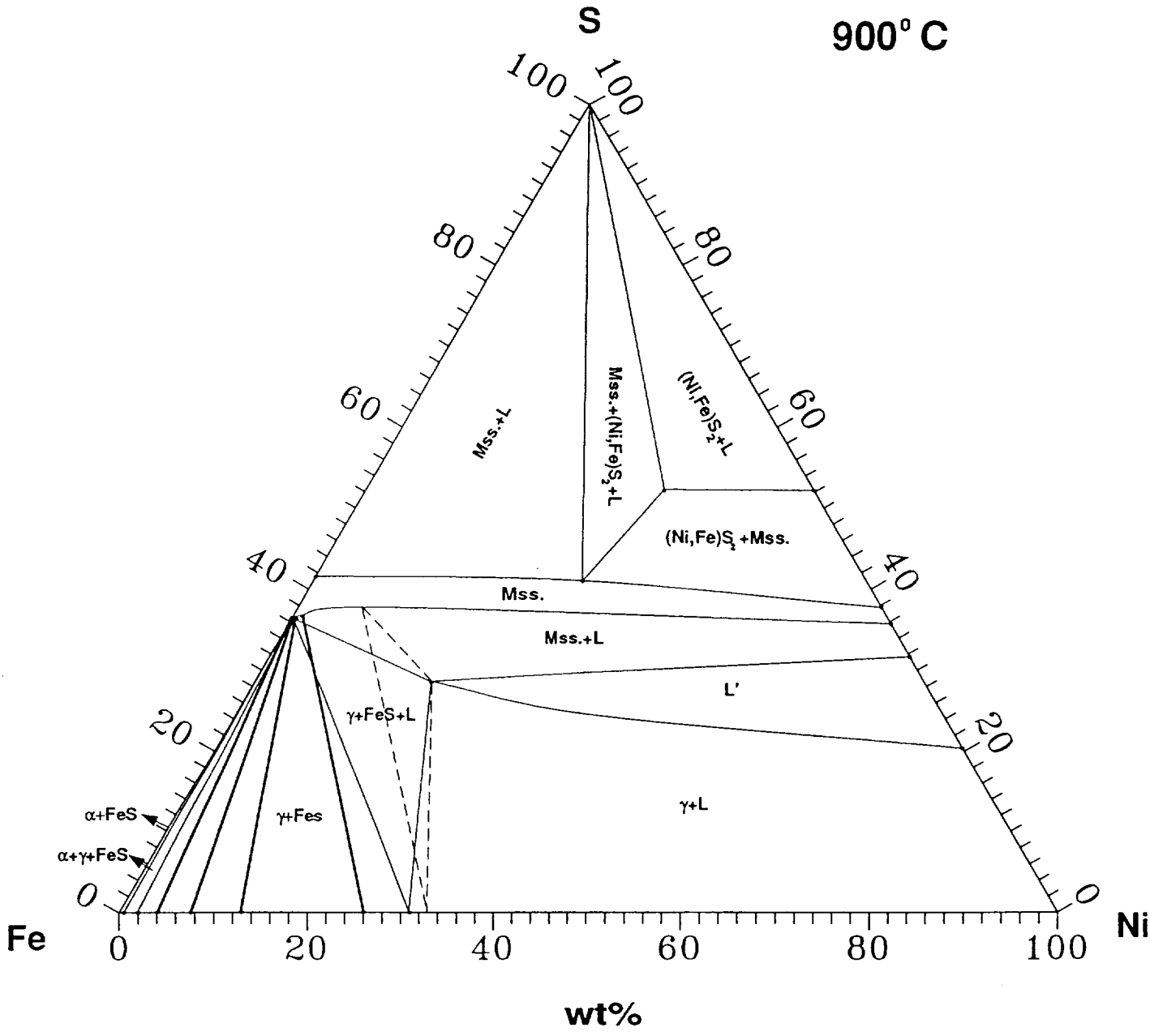

Isothermal Diagram of the Fe-Ni-S System at 900°C